Impedance Spectroscopy of α-β Tubulin Heterodimer Suspensions

Hugo Sanabria,* John H. Miller Jr.,* Andreas Mershin,† Richard F. Luduena,‡ Alexandre A. Kolomenski,§ Hans A. Schuessler,§ and Dimitri V. Nanopoulos§

*Department of Physics and Texas Center for Superconductivity at University of Houston, Houston, Texas; †Center for Biomedical Engineering, Massachusetts Institute of Technology, Cambridge, Massachusetts; ‡Center of Biochemistry, University of Texas San Antonio Health Science Center, San Antonio, Texas; and §Department of Physics, Texas A & M University, College Station, Texas

ABSTRACT Impedance spectroscopy is a technique that reveals information, such as macromolecular charges and related properties about protein suspensions and other materials. Here we report on impedance measurements over the frequency range of 1 Hz to 1 MHz of α-β tubulin heterodimers suspended in a buffer. These and other polyelectrolyte suspensions show enormous dielectric responses at low frequencies, due both to the motion of charges suspended in the medium and to an electrical double layer that forms at each electrode-medium interface. We propose an equivalent circuit model to minimize electrode polarization effects and extract the intrinsic response of the bulk medium. At megaHertz frequencies, the conductivity increases with concentration below the critical concentration of ~1 mg/ml for microtubule polymerization, above which the conductivity decreases. This suggests that such measurements can be used to monitor the dynamics of microtubule polymerization. Finally, we obtain the net charge number per tubulin dimer of $|Z| = 306$ in the saline buffer, which, if maintained as the dimers polymerized, would yield a linear charge density of 3.8 e/Å for the assembled microtubules. These results are potentially important for fundamental electrostatic processes in biomolecules and suggest the possibility of developing future bioelectronic applications.

INTRODUCTION

Recent interest in measuring the dipole moment of the α-β tubulin heterodimer under physiological conditions has spurred the development of experimental techniques to achieve this goal. Techniques that include dielectrophoresis and surface plasmon resonance (1) have been used, the latter providing a dipole moment that compares favorably to that calculated (2–4) using the 3.7 Å resolution electron crystallography structure (5). This interest is driven, in part, by the idea of using highly dipolar proteins in biological circuit design (6,7) as well as theories proposing that tubulin may act as a unit of information called a ''biobit,'' or perhaps the quantum analog of this, a ''bioqubit'' (8,9).

In vivo α-β tubulin dimers, whose dimensions are $4 \times 5 \times 8$ nm (10), polymerize to form protofilaments, which in turn combine into tubelike structures known as microtubules. Each of these hollow structures can be up to several microns long, and have ~25 nm and 14 nm outer and inner diameters. Microtubules are major components of the cellular cytoskeleton and perform numerous functions within the cell. They play critical roles in mitosis, vesicle transport, cell support, cell motility, and, possibly, information processing. Moreover, electrostatic interactions among microtubules and chromosomes in the mitotic spindle have been proposed to affect key processes, including prometaphase, metaphase, and anaphase-A (11).

The electrical properties of microtubules and their tubulin constituents have been widely studied using computational methods. Baker *et al*. (12) showed the overall negative electrostatic potential of the microtubules in an aqueous environment with small regions of positive potential, especially in the ''–'' end or slowing growing end. The ''+'' end (highly negative) corresponds to the rapidly growing end in microtubule formation.

Proteins have a complex three-dimensional structure, as well as a complex charge distribution. For example, polymers such as F-actin filaments are highly charged with a linear charge density at pH 7 of one electron charge per 2.5 Å, along its length (13,14). Another vitally important molecule is DNA, which in an aqueous environment has one electron charge per 1.7 Å. Such large charge densities can give rise to condensed structures such as charge density waves of divalent cations (14).

The theory of dielectrics, briefly reviewed below, can be used in principle to extract the dipole moment and the net charge of tubulin heterodimers suspended in a polar medium. The relative permittivity, or dielectric constant ϵ, is a measure of a system reaction to an applied electric field (15).

The experimental technique used in this study for measuring broadband frequency spectra of the relative permittivity and conductivity is relatively straightforward. By applying a sinusoidal field and sweeping the frequency over the desired range, one obtains the complex ratio of the voltage and current amplitudes, with phase information included.

Submitted July 15, 2005, and accepted for publication February 3, 2006.

Address reprint requests to John H. Miller Jr., Dept. of Physics and Texas Center for Superconductivity at the University of Houston, 4800 Calhoun Rd., Houston, TX 77204. Tel.: 713-743-8257; Fax: 713-743-8201; E-mail: jhmiller@uh.edu.

Hugo Sanabria's present address is Dept. of Neurobiology and Anatomy, University of Texas Medical School, 6431 Fannin, Rm. 7.410, MSB Houston, TX 77030.

0006-3495/06/06/4644/07 $2.00

doi: 10.1529/biophysj.106.069427

The frequency dependence of the relaxation processes will depend on the contribution of the polarizability of the material. For biological matter, there are several different frequency ranges within which one can observe these processes, including the α-, β-, and γ-relaxations. This nomenclature was first proposed by Schwan in 1957 (16). The smaller the length-scale of the relaxation process one probes, the larger the frequency is needed to observe its effect. The so-called α-response has been found to correlate with the overall membrane potentials of live whole cells in an aqueous suspension (17–19), whereas the β-response is related to the orientational polarizability of proteins and lipids. At higher frequencies, one probes smaller molecules such as amino acids and bound water until, at several GHz, attaining the γ-response that is attributed to the relaxation of individual water molecules.

Experimentally, it is quite difficult to remove parasitic effects that screen the real information. In this article, we show experimental results, a method for extracting the intrinsic properties of the medium, and an interpretation of the conductivity spectra observed for tubulin suspensions.

THEORY

Impedance spectroscopy (IS) is one of many techniques used to study the electrical properties of materials. This method has been widely used in material science, and also in studying the electrical properties of biological materials. IS is gaining renewed strength as a tool complementary to other techniques used to study the structural and related properties of proteins. Such well-established techniques include nuclear magnetic resonance, electron spin resonance, and x-ray crystallography, all of which provide important data from a structural perspective. Although IS does not have the structural selectivity of these methods, it can nevertheless provide important information about the protein's charge dynamics, as related to its structure. This method is extremely sensitive to polarization interfaces and intermolecular interactions, such as dipole-dipole interactions and cooperative processes.

The main theory of the dielectric properties of globular objects in solution is based on Onsager's theory, where a polar medium acts as the solvent and another polar substance is dissolved or suspended in it. In this theory, one considers a cavity with a permanent dipole moment in the middle. By solving the Poisson equation with the appropriate boundary conditions, it can be shown (20) that the local field plays an important role in the contribution to the field observed by the molecules. In this case, a function that relates the dipole moment of the molecules with the dielectric dispersion can be simplified to

$$\Delta\epsilon = (\epsilon_s - \epsilon_\infty) = \frac{g\mu^2 N_A C}{2\varepsilon_0 MkT}, \tag{1}$$

where μ is the dipole moment of the protein, N_A is Avogadro's number, C is the concentration in (mg/ml = kg/m^3), M is the mass of the protein (kg/mol), k is the Boltzmann constant, T the absolute temperature, and g is the (unknown) Kirkwood correlation factor, which is usually assumed to be 1. This equation tells us that, by measuring the low- and high-frequency-limiting dielectric constants, ϵ_s and ϵ_∞, one can calculate the dipole moment of the protein for given assumptions or g.

One can define the complex relative permittivity (dielectric constant) $\epsilon = \epsilon' - i\epsilon''$ as a function of the angular frequency $\omega = 2\pi f$ with the real and imaginary components,

$$\epsilon' = \epsilon_\infty + \frac{(\epsilon_s - \epsilon_\infty)}{1 + \omega^2\tau^2}, \tag{2}$$

$$\epsilon'' = \frac{\omega\tau(\epsilon_s - \epsilon_\infty)}{1 + \omega^2\tau^2}, \tag{3}$$

where τ is the inverse of the characteristic Debye relaxation frequency. In a similar way we have, for the real part of the conductivity

$$\sigma' = \sigma_s + \frac{\omega^2\tau^2(\sigma_\infty - \sigma_s)}{1 + \omega^2\tau^2}, \tag{4}$$

so that they are related by

$$(\epsilon_s - \epsilon_\infty) = \frac{\tau(\sigma_\infty - \sigma_s)}{\epsilon_0}. \tag{5}$$

Thus, by taking either the complex spectrum of the relative permittivity or the real part of the conductivity one can, in principle, extract the changes in the relative permittivity given by Eqs. 1 and 5. This relationship has been widely used for extracting with high accuracy the electrical dipole moment for other biomolecules, such as myoglobin, hemoglobin, DNA, etc. (21–23).

As the conductivity of the solution or suspension increases, the contribution from the dielectric is screened by the high concentration of ions, making the extraction of the dielectric spectrum very difficult. Under such conditions, it is better to understand the mechanisms involved in the frequency-dependent conductivity. Using the change in the high frequency limit of the conductivity (σ_∞) we can extract information about the charge density per molecule, in this case per tubulin heterodimer, which is related to the linear charge density of the polymerized microtubules. Thus, we can define the ion (charge particle) mobility u_i according to (24)

$$u_i = \frac{|Z_i|e}{\xi_i}, \tag{6}$$

where the subindex i represents the different types of ions in solution, ξ_i is the friction coefficient, and $|Z_i|$ the amount of electrical charges per ion i. For the case of an ellipsoid moving at random, we have (25)

$$\xi = \frac{6\pi\eta a}{\ln(2a/b)}, \tag{7}$$

where η is the viscosity, and the semiaxes of the ellipsoid are a and b; for the case of tubulin, they take the values of $a = 2.25$ nm and $b = 4$ nm. Then, one can relate the ion mobility to the conductivity measurements as

$$\sigma_\infty = \sum_i F|Z_i|u_i C_i = \sum_i \frac{F|Z_i|^2 eC_i}{\xi_i}, \quad (8)$$

where F is Faraday's constant.

For the experiment reported here, σ_∞ corresponds to the measured conductivity at 1 MHz and contains the contribution of both the solvent (buffer) and solute (tubulin). Then, we can rewrite Eq. 8 as

$$\sigma_\infty = \sigma_{\text{buffer}} + \sigma_{\text{tubulin}}, \quad (9)$$

where σ_{buffer} is the measured conductivity of the buffer alone at 1 MHz, and σ_{tubulin} will correspond to the contribution to the conductivity due to tubulin alone. This interpretation assumes that there is only one population of free dimers in solution and there is no aggregation effect taking place; see Results and Discussion for a better description of the use of this equation.

EXPERIMENT

To perform the impedance spectroscopy of tubulin in a buffer solution, we used a Solartron 1260 impedance analyzer (Solartron Analytical, Farnborough, UK) with a liquid cell with stainless steel electrodes, as shown in Fig. 1. The spectra were recorded from 1 Hz to 1 MHz. Polar and nonpolar liquids were used for calibration purposes, for which the real part of the relative permittivities (ϵ') are shown in Fig. 2. It is clear from this data that polar liquids increase the electrode polarization effects at lower frequencies. Several methods exist to compensate such electrode polarization effects, which can be thought of as the appearance of a small diffusive (or double) layer, a few molecules thick, which screens the electric field and thus gives an apparent increase in the measured capacitance. Some of the proposed methods include changing the spacing between the electrodes and assuming that the additional impedance due to electrode polarization is independent of the separation distance (17). This method works best for separation distances that are large compared to the diameter of the electrode. For the measurements reported here we are restricted by the small sample volume, and thus this technique is not satisfactory.

An alternative method is to consider modeling the double-layer effect on the circuit, as shown in Fig. 3, where we have used a constant phase element (CPE) to represent the polarization impedance Z_p. Let us recall that the impedance of the CPE is written as

$$Z_p = \frac{1}{Q(i\omega)^p}, \quad (10)$$

where Q can be considered as a measure of the concentration of ions close to the interface between the electrode and the electrolyte and p has been called the fractal dimension (26); it is related to the roughness of the electrode surface (27,28). Its fractal nature takes into account the porosity of the electrode, which is the main difference as compared to a simple capacitive layer, corresponding to $p = 1$. The thickness of this porous layer contributing to the polarization impedance is related to the Debye length. Also such power law behavior can be obtained by assuming a random walk of ions near to the rough surface of the electrode (29).

For the case of polar molecules, we use Eq. 10 to account for the large contribution of the polarization effect, thus the total impedance is given by

$$Z(\omega) = R_s + i\omega L_s + \frac{1}{Q(i\omega)^p} + \frac{1}{1/R_m + i\omega C_m}, \quad (11)$$

where $R_s + i\omega L_s$ corresponds to the cable impedance; the next term is the CPE polarization impedance described above; and the last term is the leakage capacitor described by a pure capacitor $C_m = \epsilon'\epsilon_0 A/d$ (with A the surface area of the electrode and d the separation distance) connected in parallel with a resistor $R_m = i/G_m$, where $G_m = \sigma' A/d$ is the conductance.

Using Eq. 11, one can obtain a good fit for the data shown in Fig. 2, where the measured points are shown by symbols

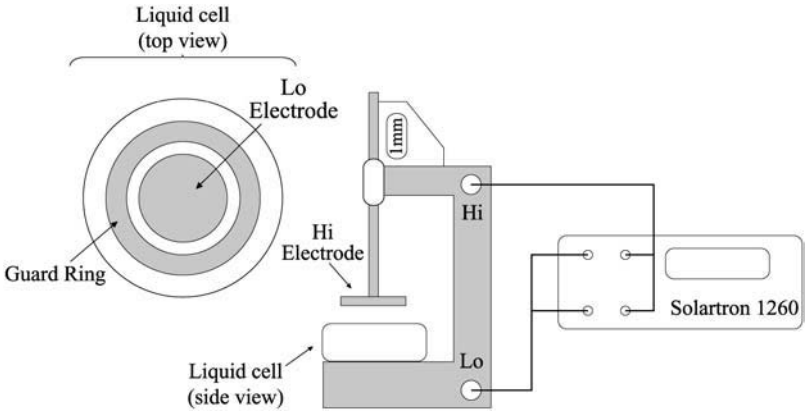

FIGURE 1 Experimental setup. A Solartron 1260 impedance analyzer was used to sweep the frequency from 1 Hz to 1 MHz. The liquid cell with stainless steel electrodes was 2 cm in diameter, and contained a guard ring that reduced fringing fields. The separation distance used in the experiments between the electrodes was 1 mm.

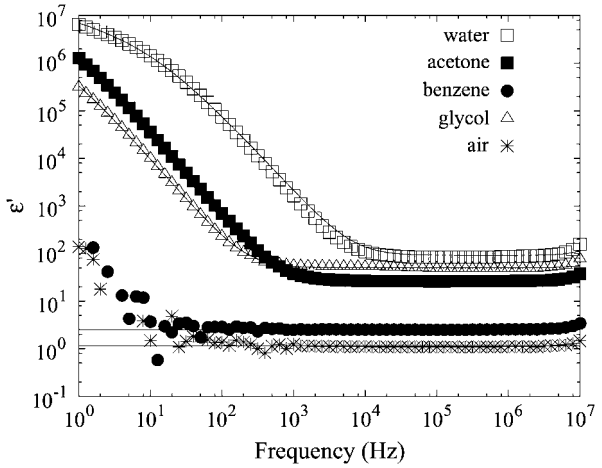

FIGURE 2 Calibration curves for polar and nonpolar liquids. For nonpolar liquids, we used a simple model, that includes a leakage capacitor to fit the data with the solid lines (Parallel RC circuit). For polar liquids we fit the data using Eq. 11 with the constant phase element as a model for the polarization effect.

and their correspondent model fitting shown in solid lines. The difference between the fitting of polar liquids (water, glycol, and acetone) and nonpolar (benzene, air) is that, for nonpolar liquids, the polarization impedance and cable impedance are neglected. In these cases, the capacitance is constant, as shown for benzene and air, with good agreement with the reported values (30). Polar liquids, as well as ionic solutions, have strong polarization effects at the electrode interfaces; therefore, the model for them includes all the terms in Eq. 11. In addition, liquids with large conductivity impede the measurement of the relative permittivity of the sample, because most of the contribution to the impedance will be given by ionic currents.

METHODS

Tubulin was purified from bovine cerebra and rapidly frozen (31). It was kept at −80°C for further use at a concentration of 6 mg/ml in buffer solutions composed of 0.1 M MES, 1 mM EGTA, 0.1 mM EDTA, 0.5 mM $MgCl_2$, and 1 mM GTP at a pH 6.4. The experiment started with the highest concentration of 2 mg/ml with the initial volume 1.5 ml. We allowed samples to reach room temperature and then waited 45 min before taking measurements, allowing time for polymerization that was expected to occur at concentrations above 1.1 mg/ml. The complex impedance of each suspension was measured over the frequency range of 1 Hz to 1 MHz, and then the buffer solution was added and resuspended by pipetting to change the concentration in steps of 0.1 mg/ml until reaching a final concentration of 0.1mg/ml.

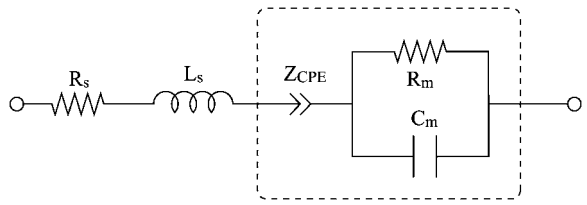

FIGURE 3 Circuit model. In this model, we included the cable impedance as well as the constant phase element to correct for the polarization effect.

It is known that the tubulin dimers spontaneously polymerize when their concentration exceeds a critical concentration of ~1.0 mg/ml (10). Also, this process is reversible and will only depend, for a few polymerization cycles, on the concentration of tubulin. In addition, studies of the temperature dependence of polymerization show that, at temperatures below 4°C, mammalian tubulin cannot polymerize and form microtubules.

RESULTS AND DISCUSSION

For calibration of the liquid cell we measured a short terminus, for which one can evaluate the parasitic effect of the cable impedance ($R_s = 0.33\ \Omega$ and $L_s = 2 \times 10^{-7}$ H), and subtracted it from the data. From the model used we observed that the conductivity of the buffer was high, because of the amount of ions in the solution and with addition of tubulin the conductivity changed drastically.

By fitting the data with the model described by Eq. 11, as in the case of the calibration data (Fig. 2), we obtained the exponent in the CPE element, sometimes called fractal dimension, for each concentration, with a mean value of 0.85 (see Fig. 4). This value is close to the previously reported of 0.78 for stainless steel electrodes (26), the difference is attributed only to changes in surface roughness, having in mind that when $p = 1$ the surface is considered to be perfectly flat. The parameter Q shows an increase with tubulin concentration (Fig. 5).

In addition, we extracted the real part of the conductivity versus frequency of tubulin suspensions. This was obtained after subtracting the constant phase-angle impedance and other external impedance elements shown in Fig. 6. Here we observed a relaxation process at ~1 kHz mainly due to the motion of ions at the electrode interface (H. Sanabria and J. H. Miller Jr., unpublished work); this relaxation process is

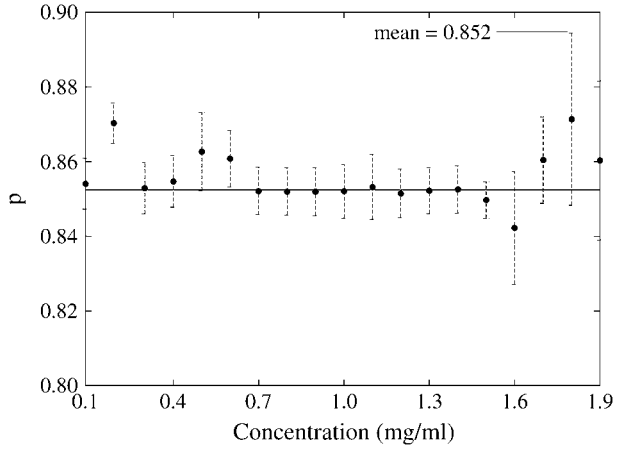

FIGURE 4 Variation of fitted parameter p from Eq. 10 with respect to changes in concentration, showing that the fractal dimension does not change considerably.

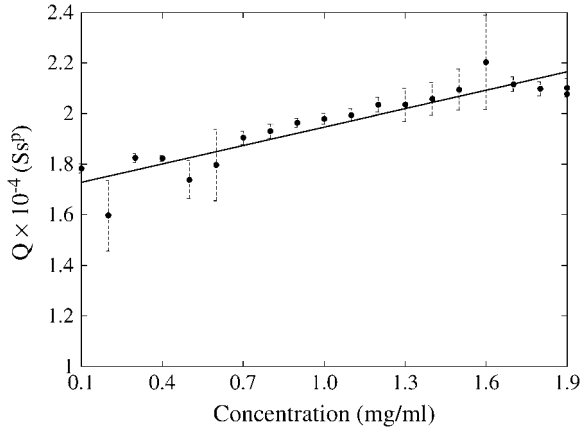

FIGURE 5 Linear change of the parameter Q with respect to the concentration of tubulin in suspension.

described by Eq. 4. Since the capacitive effects of the sample were screened by the high conductivity of our solution in this case, it was better to work with the conductivity spectra in which we have observed changes with respect to the concentration. In addition, Fig. 6 shows the difference in the conductivity measurements between a buffer solution with no tubulin and with tubulin at various concentrations. This difference gives almost a twofold increment in the conductivity, which is related to the large charge expected of tubulin dimers.

The increase of the high frequency limit of conductivity (σ_∞), obtained below the critical concentration of 1.1 mg/ml shown in Fig. 7 from fitting Eq. 4 to the tubulin solutions, is due to the fact that tubulin itself is negatively charged, giving rise to more charge particles in motion in our solution. It should be noted that the conductivity versus concentration reaches a maximum near the critical concentration, where tubulin dimers start polymerizing to form microtubules.

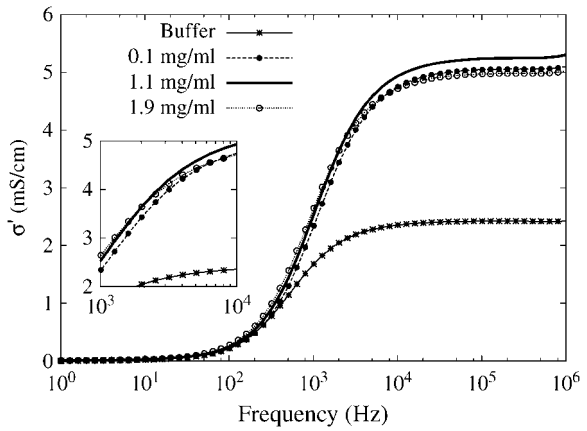

FIGURE 6 Conductivity spectra for tubulin suspensions. The relaxation frequency observed in the kHz range is mainly due to the accumulation of ions at the interface. The inset shows, in detail, the frequencies between 1 and 10 kHz.

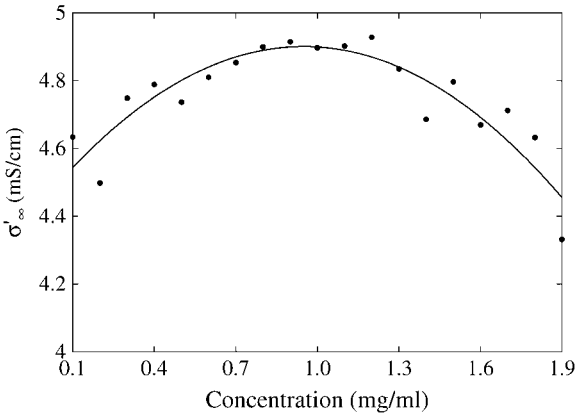

FIGURE 7 Behavior of σ'_∞ as a function of the concentration after 45 min. The maximum point in the trend line is close to the 1.1 mg/ml, which is the critical concentration at which microtubules start polymerizing. After polymerizing above this concentration, they exhibit the well-known dynamic instability.

Microtubule polymerization most likely affects the conductivity of the sample, because the mobility of the microtubules is smaller than that of the tubulin dimers. In addition, after they polymerize, they will also enter into an active phase where microtubules show dynamic instability.

To calculate the net charge per dimer, we can consider Eq. 8 as the sum of the conductivity of the buffer, which contains all of the different constituents, plus the conductivity of the tubulin dimers. This assumption is only valid in the region where there is no polymerization, because as we have shown at the critical concentration the conductivity is not linear.

Solving for $|Z|$ from Eq. 8 the amount of charge per tubulin dimer is given by

$$|Z| = \left(\frac{\sigma_{\text{tubulin}} 6\pi\eta a}{eFC\ln(2a/b)}\right)^{1/2}. \tag{12}$$

In SI units, the concentration of tubulin used was $C = 0.011$ mol/m^3, Faraday constant is 96485.3 C/mol, the viscosity of the buffer is assumed to be close to that of the water 1 cP $= 0.001$ Ns/m^2, and the change in the limiting high frequency of the conductivity from a concentration of 0.1 mg/ml to buffer alone is $\sigma_{\text{tubulin}} = \sigma_\infty - \sigma_{\text{buffer}} \sim 0.24$ S/m. This calculation gives a net charge $|Z| \sim 306$ at pH 6.4, which is within an order of magnitude, but significantly higher than the reported value of ~ -20 at pH 6.5 for no salts and no intramolecular charge compensation (32). The net charge obtained when divided by the length of the dimer yields a linear charge density for the microtubules of $\sim$3.8 e/Å. This is considering the microtubules to be as one-dimensional wires, but most certainly all the charge is distributed in a nonhomogeneous manner over the whole surface/volume of the microtubules yet to be resolved.

In addition, there are several considerations or assumptions for which we obtained such a large value for $|Z| \sim 306$

electrical charges per dimer, including the fact that Eq. 12 takes the difference on conductivity from buffer alone and with a defined concentration. If one follows the quadratic behavior observed on the fitted curve in Fig. 7, and finds the limit when there is no tubulin present in solution, the difference in conductivity is an order-of-magnitude less σ_{tubulin} 0.02 S/m, giving an order-of-magnitude less on the total electrical charges $|Z| \sim 30$.

Also, it is worthwhile to mention that Eqs. 8 and 9 do not consider the right population statistics of pure tubulin and the population of microtubules formed—affecting the contribution to the conductivity of the free dimers, which are the more mobile inside the solution. Such consideration can only give us, for the time being, a range of the charge density to be from 0.3 to 4 e/Å. Obviously, the lower limit gives a better agreement with the values previously reported (32).

Other factors are present that will affect the expected charge density; these include enhanced viscosity of the tubulin suspension as compared to that of water (33), which affects the mobility of the dimers in suspension, as well as the presence of cations and anions that interact with the tubulin dimers to create a charged shroud surrounding each isolated dimer. When the dimers polymerize to form microtubules, the areas of the regions in contact with the electrolyte will be greatly reduced, which would tend to greatly reduce the total charge of the ''shroud.'' Another factor that may play a role is a possible preferred orientation of the dimers when they move in response to an applied field.

CONCLUSIONS

Impedance spectroscopy has been used to obtain electrical properties such as net charge of tubulin in solution. Recent the interest on learning more about the dynamics of tubulin makes this technique very promising, because it is very sensitive to polarization effects, molecular interactions like dipole-dipole interactions, and cooperative processes.

There are experimental artifacts at low frequencies that have to be considered, such as electrode polarization, which screen the information and make the data analysis difficult. Such effects cannot be removed completely, but can be reduced using various approaches, some of which include changing the separation distance of the plates, using four-electrode techniques or the approach used in this article by including a constant phase element accounting for a fractal behavior of the electrodes in the circuit model.

We have shown that the dynamics of polymerization can be studied using impedance spectroscopy, a technique that seems promising for future studies of the dynamics of proteins, including the study of conformational changes. Also we were able to extract a linear charge density for microtubules of 3.8 e/Å, which may be important for fundamental electrostatic processes and suggests the possibility of developing future bioelectronic applications.

We thank Veena Prasad for purifying the tubulin used in this study and for her skilled technical assistance.

This work was partially supported by the Texas Center for Superconductivity at the University of Houston, by the Robert A. Welch foundation (grant No. E-1221), and by the Institute for Space Systems Operation. Additional partial support was provided by a National Science Foundation grant (No. 0218595), a grant from the Telecommunications and Informatics Task Force from Texas A&M University, and by grants to R.F.L. from the Welch Foundation (No. AQ-0726), the US Army Prostate Cancer Research Program (No. W81XWH-04-1-0231), and the US Army Breast Cancer Research Program (No. W81XWH-05-1-0238).

REFERENCES

1. Lioubimov, V., A. A. Kolomenski, A. Mershin, D. V. Nanopoulos, and H. A. Shuessler. 2004. Effect of varying electric potential on surface-plasmon resonance sensing. *Appl. Opt.* 43:3426–3432.
2. Brown, J. A. 1999. A study of the interactions between electromagnetic fields and microtubules: ferroelectric effects, signal transduction and electronic conduction. Ph.D. thesis, University of Alberta.
3. Brown, J. A., and J. Tuszynski. 1997. Dipole interactions in axonal microtubules as a mechanism of signal propagation. *Phys. Rev. E.* 56: 5834–5840.
4. Mershin, A., A. A. Kolomenski, H. A. Shuessler, and D. V. Nanopoulos. 2004. Tubulin dipole moment, dielectric constant and quantum behavior: computer simulations, experimental results and suggestions. *Biosystems.* 7:73–85.
5. Nogales, E., S. G. Wolf, and K. H. Downing. 1998. Structure of the α-β tubulin dimer by electron crystallography. *Nature.* 391:199–203.
6. Muthukrishnan, G., C. A. Roberts, Y. C. Chen, J. D. Zahn, and W. O. Hancock. 2004. Patterning surface-bound microtubules through reversible DNA hybridization. *Nano Lett.* 4:2127–2132.
7. Moorjani, S. G., L. Jia, T. N. Jackson, and W. O. Hancock. 2003. Lithographically patterned channels spatially segregate kinesin motor activity and effectively guide microtubule movements. *Nano Lett.* 3:633–637.
8. Mavromatos, N. E., and D. V. Nanopoulos. 1998. On quantum mechanical aspects of microtubules. *Int. J. Mod. Phys.* B12:517–542.
9. Mershin, A., H. Sanabria, J. H. Miller, Jr., D. Nawarathna, E. M. Skoulakis, N. E. Mavromatos, A. A. Kolomenskii, H. A. Schuessler, R. F. Luduena, and D. V. Nanopoulos. 2005. Towards experimental tests of quantum effects in cytoskeletal proteins. *arXiv:physics/0505080.*
10. Tuszynski, J. A., and M. Kurzynski. 2003. Introduction to Molecular Biophysics. CRC Press, Boca Raton, FL.
11. Gagliardi, L. J. 2005. Electrostatic force generation in chromosome motions during mitosis. *J. Electrostatics.* 63:309–327.
12. Baker, N. A., D. Sept, S. Joseph, M. J. Holst, and J. A. McCammon. 2001. Electrostatics of nanosystems: application to microtubules and the ribosome. *Proc. Natl. Acad. Sci. USA.* 98:10037–10041.
13. Tuszynski, J. A., S. Portet, J. M. Dixon, C. Luxford, and H. F. Cantiello. 2004. Ionic wave propagation along actin filaments. *Biophys. J.* 86:1890–1903.
14. Angelin, T. E., H. Liang, W. Wriggers, and G. C. L. Wong. 2003. Like-charge attraction between polyelectrolytes induced by counterion charge density waves. *Proc. Natl. Acad. Sci. USA.* 100:8634–8637.
15. Feynman, R. P., R. B. Leighton, and M. Sands. 1977. The Feynman Lectures on Physics, Vol. 2. Addison-Wesley, Reading, MA.
16. Schwan, H. P. 1958. Advances in Biological and Medical Physics. Academic Press, New York.
17. Prodan, C. 2003. Dielectric properties of live cells in suspension. Ph.D. thesis, University of Houston.
18. Gheorghiu, E. 1993. The resting potential in relation to the equivalent complex permittivity of a spherical cell suspension. *Phys. Med. Biol.* 38:979–988.

19. Gheorghiu, E. 1994. The dielectric behaviour of suspensions of spherical cells: a unitary approach. *J. Phys. A Math. G E N.* 27:3883–3893.

20. Onsager, L. 1936. Electric moments of molecules in liquids. *J. Am. Chem. Soc.* 58:1486–1493.

21. Grant, E. H., R. Sheppard, and G. South. 1978. Dielectric Behavior of Biological Molecules in Solution. Oxford University Press, New York.

22. Cohn, E. J., and J. T. Edsall. 1943. Proteins, Amino Acids and Peptides. Reinhold Publishing, New York.

23. Ermolina, I. V., I. N. Ivoylov, and V. D. Fedotov. 1997. Dielectric relaxation, molecular motion and interprotein interactions in myoglobin solutions. *J. Biomol. Struct.* 15:381–392.

24. Bard, A. J., and L. R. Faulkner. 1980. Electrochemical Methods: Fundamentals and Applications. Wiley, New York.

25. Berg, H. C. 1993. Random Walks in Biology. Princeton University Press, Princeton, NJ.

26. Feldman, Y., R. Nigmatullin, E. Polygalov, and J. Texter. 1998. Fractal-polarization correction in time domain dielectric spectroscopy. *Phys. Rev. E.* 58:7561–7565.

27. Kim, C., S. Pyun, and J. Kim. 2003. An investigation of the capacitance dispersion on the fractal carbon electrode with edge and basal orientations. *Electrochim. Acta.* 48:3455–3463.

28. Pajkossy, T., and L. Nyikos. 1990. Scaling-law analysis to describe the impedance behavior of fractal electrodes. *Phys. Rev. B.* 42:709–719.

29. Halsey, T. C., and M. Leibig. 1992. The double layer impedance at a rough surface: theoretical results. *Ann. Phys.* (*NY.*) 219:109–147.

30. Ride, D. L. 2004–2005. CRC Handbook of Chemistry and Physics, 85th Ed. CRC Press, Boca Raton, FL.

31. Fellous, A., J. Francon, A.-M. Lennon, and J. Nunez. 1977. Microtubule assembly in vitro. Purification of assembly-promoting factors. *Eur. J. Biochem.* 78:167–174.

32. Tuszynski, J. A., J. A. Brown, E. Crawford, E. J. Carpenter, M. L. A. Nip, J. M. Nixon, and M. V. Sataric. 2005. Molecular dynamics simulations of tubulin structure and calculations of electrostatic properties of microtubules. *Math. Comput. Mod.* 41:1055–1070.

33. Howard, J. 2001. Mechanics of Motor Proteins and the Cytoskeleton. Sinauer Associates, Sunderland, MA.